The Chiral Phase Transition of the hot QCD from the Exact Renormalization Group

Dai SHIMIZUBE[1,*] and Jun-Ichi. SUMI[2, **]

[1]*Graduate School of Human and Environmental Studies, Kyoto University*
Yoshida, Kyoto University, Kyoto 606-8501, Japan
[2]*Riverroad Takano 221, Ooharada-cho 8, Ichijoji, Sakyo-ku,*
Kyoto 606-8187, Japan

Abstract

The chiral phase transition of the finite temperature QCD is discussed in the ladder approximated Exact (Wilson's) Renormalization Group (ERG). The gluon thermal mass is incorporated by the Hard Thermal Loop (HTL) approximation. We calculated a critical temperature T_c, a critical exponent ν, and order parameters such as chiral condensate $<\bar{\psi}\psi>$ and pion decay constants with this approximation. The dependences of the pion decay constants on an unphysical parameter are fairly improved by including contributions from momentum dependent vertices. The critical temperature was found as: $T_c \approx 124$ MeV for 3-flavors. It was shown that the critical temperature considerably depends on the approximation scheme for the gluon thermal mass term. We also calculated the temperature dependence of the chiral condensate, π decay constants, and the pion velocity.

*) E-mail address: simizube@phys.h.kyoto-u.ac.jp
**) E-mail address: j-sumi@blue.vecceed.ne.jp

typeset using $\mathcal{PTP}$TEX.cls ⟨Ver.0.9⟩

§1. Introduction

Explorations of the chiral nature of QCD at high temperature are experimental as well as theoretical interests. They are relevant to the early universe and to the heavy ion collisions at RHIC and those planned at LHC. It is believed that the approximate chiral symmetry observed at bare Lagrangian dynamically breaks down at zero temperature due to the chiral condensate contained in the QCD vacuum. At high temperature, the chiral condensate is expected to melt, and the chiral symmetry is restored at a certain critical temperature. Since the perturbative methods can not be applied to the non-trivial QCD vacuum, so we need non-perturbative methods, such as the lattice Monte-Carlo simulation, the Schwinger-Dyson equation, and the Exact Renormalization Group, for investigating the vacuum structure of QCD at high temperature.

For the zero temperature case, the Schwinger-Dyson equations (SDEs) has been studied[1]-[4] and has been applied to the strong coupled QED and QCD.[5]-[7] Commonly, the so-called (improved) ladder approximation[5] has been applied to solve the SDEs. Although these approximation schemes seem to be fairly crude, the SDEs offer surprisingly good results on the dynamical chiral symmetry breaking in QCD. For the finite temperature gauge theories, the SDEs were also applied.[8]-[14] At finite temperature, the gauge interaction is corrected by thermal effects. Thermal effects, such as the Debye screening and the Landau damping, appear in the gauge boson propagator as their thermal mass. So it is no longer to say that how to approximate the thermal mass is one of the main subjects for the improvement of finite temperature analyses. The hot QED was discussed in the instantaneous-exchange (IE) approximation for the gauge boson propagator including the screening effect in the static limit,[8] or the IE approximation for the longitudinal (electric) mode and the Hard Thermal Loop Approximation for transverse (magnetic) modes.[9] The chiral phase transition of the hot QCD was studied by neglecting the gluon thermal/Debye mass term.[10]-[12] The Phase structure of hot and/or dense QCD was explored by introducing the Debye mass in static limit of the gluon propagator.[13] However unfortunately the improvement of the above approximations seems to be difficult due to the complexity of the integral equation.

The Exact Renormalization Group (ERG) has been applied to investigate the chiral nature of the strong coupling gauge theory at zero temperature.[15] With ERG method, we can study the chiral critical behavior in very simple manner, and if we approximate the ERG flow equations to the ladder-like corrections then it leads the identical results with those obtained by solving the ladder SDEs. It should be noted that we can improve the approximation scheme systematically, e.g. incorporating the "crossed-ladder" diagrams. Especially, the large gauge dependence of the solutions obtained by the ladder SDEs[16] has

been improved in the case of the chiral critical behavior in QED.[17]

For the finite temperature, the chiral nature has been investigated by the "Quark-Meson model" in ERG method.[18] The Quark-Meson model is defined at 'so-called' compositeness scale $k_\Phi \approx 600$ MeV from the zero temperature QCD and therefore does not incorporate the thermal screening of the gluon interaction. It is expected that the mesonic bound states forms at the short scale region: $k > k_\Phi$ and are not affected by the long distance: $k < k_\Phi$ behavior of the gluon propagator. It is one of the issue whether the thermal screening effect to the chiral behavior can be neglected or not.

In this paper, we investigate the chiral phase transition of the hot QCD in the ladder approximation with including the gluon thermal mass in the Hard Thermal Loop (HTL) approximation. To introduce auxiliary fields, we consider a intermediate momentum scale similar to k_Φ in the Quark-Meson model. The pion decay constants depend on the intermediate scale, which is an unphysical parameter. By including contributions from momentum dependent vertices, the decay constants become considerably stable for the intermediate scale. The formation of the chiral condensate is remarkably affected by the thermal screening. Especially, the critical temperature is remarkably lowered in comparison with that given by neglecting the thermal mass. We also calculated the temperature dependence of the order parameters, i.e. the chiral condensate and the pion decay constants for several approximation schemes for the thermal mass.

We estimated the temperature dependence of the pion velocity too, from the ratio of the spatial component of the decay constant and the temporal component of that, which become different at finite temperature.[19] By the ladder approximated SDE, the temperature dependence of the 'space-time averaged' component of the pion decay constant was evaluated,[11] however, that of the pion velocity was not. It is expected that pions travel at less than the speed of light in a thermal bath. In this paper, it is shown that pions are slowed down slightly near T_c.

This paper is organized as follows. We explain our approximation scheme and derive the ERG flow equations in §2. In §3 we show the numerical results. §4 is devoted to the summary and discussions.

§2. The ERG equation

In this section we explain the approximation scheme first, and next we derive the ERG equation. Let us start form N_f-flavor QCD at finite temperature T. The bare Lagrangian

density $\mathcal{L}$ is given by

$$\mathcal{L} = \frac{1}{4}\mathbf{tr}F_{\mu\nu}F^{\mu\nu} + \bar{q}i\not{D}q + \frac{1}{2\alpha}\left(\partial_\mu A_\mu^A\right)^2 + \partial_\mu \bar{C}^A \left[\partial_\mu \delta_{AB} + gf_{ABC}A_\mu^C\right]C_B, \qquad (2\cdot1)$$

where q denotes the $N_f \times N_c$ components quarks. N_c is the number of color. The field strength $F_{\mu\nu} = F_{\mu\nu}^A T^A$ and the covariant derivative D_μ are given by,

$$D_\mu = \partial_\mu + igA_\mu^A T^A, \qquad (2\cdot2)$$

$$F_{\mu\nu}^A = \partial_\mu A_\nu^A - \partial_\nu A_\mu^A + gf_{ABC}A_\mu^C A_\nu^B. \qquad (2\cdot3)$$

The third term is gauge fixing one, and the fourth is from FP ghosts. We choose the Landau gauge $\alpha = 0$. Here $\mathcal{L}$ is invariant under the chiral flavor symmetry $U_R(N_f) \times U_L(N_f)^{*)}$. The axial current is defined as $J_{5\mu}^a \equiv \bar{q}\gamma_\mu\gamma_5\lambda^a q$, where a denotes iso-spin indices and λ^a are the generators of the chiral $U(N_f)$ ($\mathbf{tr}\lambda^a\lambda^b = \frac{1}{2}\delta^{ab}$).

2.1. Gauge interaction

There are some problems in the application of the ERG to the gauge theory because of the infrared cutoff term which explicitly breaks gauge invariance.[20),21)] There are two ways to treat the gauge theory. One is generalizing the ERG keeping the gauge symmetry.[21)] This is of course an ideal method, however their formulations are not accompanied with the non-perturbative approximation method. The other is introducing the gauge non-invariant counter terms to compensate the gauge invariance. Hence, the bare action does not satisfy the Slavnov-Taylor Identity, but Modified one.[20)] However, since we would like to introduce the gluon self energy in the HTL approximation, we must calculate the momentum dependent gluon self energy and therefore relevant terms of the Modified Slavnov-Taylor Identity (MSTI) become complicated integral equations.

In this paper, we do not adopt the either methods explained above. We integrate out gluons at the beginning and solve ERG flow equations for the reduced fermionic theory. This procedure generally causes many multi-fermi interactions. By the diagrammatical consideration, one can easily realize that all ladder type diagrams are generated by only the four fermi operator induced by the one gluon exchange. Other multi fermi operators generate the non-ladder diagrams. So as shown in Fig. 1, we replace the gauge sector with the non-local four fermi interaction induced by the one gluon exchange i.e.

$$G_1 \equiv \int_q \int_p \int_k g(p,k)g(q,-q-p-k)\bar{q}(k)\gamma_\mu T^A q(p)D_{\mu\nu}^{AB}(p+k)\bar{q}(q)\gamma_\nu T^B q(-q-p-k), \quad (2\cdot4)$$
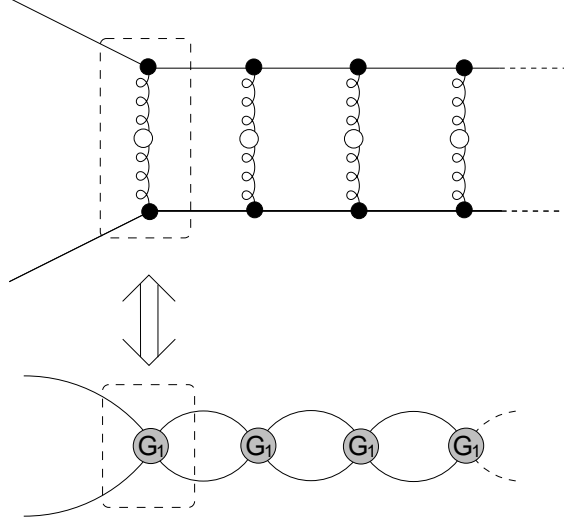
Fig. 1. 1-gluon exchange as 4-fermi interaction in the ladder approximation.

where $g(p, k)$ and $D_{\mu\nu}^{AB}$ are the running gauge coupling constant and the gluon propagator respectively. Note that, since other corrections from the gluon fluctuations do not contribute to the ladder approximation, our treatment does not mean the additional approximation. Now, what we should investigate is reduced to the fermionic theory interacting through the non-local four fermi interaction (2·4) and the ladder approximate solutions can be found in the leading order of $1/N_c$ expansion with the coupling constant $\bar{g}$: $g^2 \equiv \bar{g}^2/N_c$.

The flow of the momentum dependent four fermi interaction is studied by Meggiolaro et al.[22] They do not integrate out gluons at the beginning. They introduce the IR cutoff term for gluons and the ERG flow starts from the QCD classical action. In their work, to compensate the gauge invariance, the gluon mass is given so as to satisfy the MSTI at the leading perturbative order. We do not examine the flow of such interactions themselves as they did, but the flow of the effective potential V. The contribution from the momentum dependent four fermi interaction appears in the ERG equation for V and affects the chiral transition, in which we are interested.

The argument of the gauge coupling constant should be taken as $g(p, k) = g((p+k)^2)$ to satisfy the chiral Ward identities.[23] The infrared singularity of the gauge coupling constant is regularized as :

$$
g^2(\Lambda) = \begin{cases} \frac{1}{b \ln(\Lambda^2/\Lambda_{\mathrm{QCD}}^2)} & \text{if } \Lambda > \Lambda_1 \\ \frac{1}{b \ln(\Lambda_1^2/\Lambda_{\mathrm{QCD}}^2)} + \frac{\left((\ln(\Lambda_2/\Lambda))^2 - (\ln(\Lambda_2/\Lambda_1))^2\right)}{b \ln(\Lambda_2/\Lambda_1)(\ln(\Lambda_1^2/\Lambda_{\mathrm{QCD}}^2))^2} & \text{if } \Lambda_1 \geq \Lambda > \Lambda_2 \\ \frac{1}{b \ln(\Lambda_1^2/\Lambda_{\mathrm{QCD}}^2)} - \frac{\ln(\Lambda_2/\Lambda_1)}{b(\ln(\Lambda_1^2/\Lambda_{\mathrm{QCD}}^2))^2} & \text{if } \Lambda \leq \Lambda_2 \end{cases} \tag{2·5}
$$

where $\ln(\Lambda_1/\Lambda_{\mathrm{QCD}}) = 0.25$, $\ln(\Lambda_2/\Lambda_{\mathrm{QCD}}) = -1.0$ and $b = (11N_c - 2N_f)/48\pi^2$.

At high temperature gluons become massive by the thermal fluctuation. We incorporate the Debye-screening effect to the gluon propagator $D_{\mu\nu}^{AB}$ in the HTL approximation. Of course, the HTL approximation is based on the perturbative QCD and it is valid in the high energy (short distance) region. However, it is expectable that the short distance behavior is important to the QCD chiral physics, not the long distance one. Also, it is known that the order parameters, such as the chiral condensate, hardly depend on the difference of the treatments of the running coupling constant in the low energy region.[7] So applying the HTL approximation for the gluon propagator is a proper procedure for our present purpose, which is the first step of the improvement of the approximation for introducing thermal effects. Of course it should be checked that how order parameters and the critical temperature depend on the IR cutoff scheme for $g(\Lambda)$ at finite T. We show the Λ_1 dependence of our numerical results later, in §3.

The gluon self-energy is a gauge dependent quantity, contrary to the photon self-energy in QED. However the HTL approximated one has no dependence on the choice of gauge. At finite temperature, the self-energy matrix takes the following form:

$$\Pi_{\mu\nu}^{AB} = \left(F P_{\mu\nu}^L + G P_{\mu\nu}^T \right) \delta^{AB}. \tag{2·6}$$

The projectors $P_{\mu\nu}^L$ and $P_{\mu\nu}^T$ are given by

$$P_{\mu\nu}^T = \bar{\delta}_{\mu\nu} - \frac{\bar{p}_\mu \bar{p}_\nu}{\bar{p}^2}, \quad P_{\mu\nu}^L = \delta_{\mu\nu} - \frac{p_\mu p_\nu}{p^2} - P_{\mu\nu}^T. \tag{2·7}$$

We use the following notation, $\bar{p}_\mu = (0, \vec{p})$ and $\bar{\delta}_{\mu\nu} = \text{diag}(0, 1, 1, 1)$. One can easily verify that $P_{\mu\mu}^T = 2, P_{\mu\mu}^L = 1$. In the HTL approximation, F and G take the form:[24]

$$F = p^2 + \frac{p^2}{\bar{p}^2} \Pi_{00}(p_0, \bar{p}) = p^2 + m_{\text{HTL}}^2 (\eta^2 - 1) \Phi(\eta), \tag{2·8}$$

$$G = p^2 + \frac{1}{2} \Pi_{ii}(p_0, \bar{p}) - \frac{p_0^2}{2\bar{p}^2} \Pi_{00}(p_0, \bar{p}) = p^2 + \frac{1}{2} m_{\text{HTL}}^2 \left[1 - (\eta^2 - 1) \Phi(\eta) \right], \tag{2·9}$$

where $\eta = ip_0/|\bar{p}|$. At temperature T, the thermal mass m_{HTL} and $\Phi(\eta)$ are given by

$$m_{\text{HTL}}^2 = \frac{1}{3} g^2 T^2 \left(N_c + \frac{1}{2} N_f \right), \tag{2·10}$$

$$\Phi(\eta) = \frac{\eta}{2} \ln \left(\frac{\eta + 1}{\eta - 1} \right) - 1$$

$$= \frac{p_0}{|\bar{p}|} \tan^{-1} \frac{|\bar{p}|}{p_0} - 1. \tag{2·11}$$

6

2.2. The auxiliary fields

It is convenient to introduce the auxiliary fields for the quark-antiquark pairs to make calculation efficient.[15] We introduce the auxiliary fields for the composite operators $\bar{q}_{\Lambda_{\mathrm{AUX}}} q_{\Lambda_{\mathrm{AUX}}}$ and $i\bar{q}_{\Lambda_{\mathrm{AUX}}} \gamma_5 q_{\Lambda_{\mathrm{AUX}}}$, where $q_{\Lambda_{\mathrm{AUX}}}$ is the low energy mode of the quarks defined by

$$q_{\Lambda_{\mathrm{AUX}}}(x) = T \sum_n \int \frac{d^3 \mathbf{p}}{(2\pi)^3} q_i(\mathbf{p}) e^{ipx} \theta(\Lambda_{\mathrm{AUX}} - p). \tag{2.12}$$

The q_0 integral reduces to the Matsubara sum, i.e. $q_0 \to 2(n+1)\pi T, n = 0, \pm 1, \pm 2, \cdots$. The intermediate momentum scale Λ_{AUX} plays similar role to the compositeness scale k_Φ in Ref.18). However we do not impose the compositeness conditions[25] at this scale.

The auxiliary fields σ and π are introduced by inserting the following trivial Gaussian integrals:

$$1 = \mathcal{N}^{-1} \int D\sigma \exp\left\{ -\frac{1}{2} M^2 \int_0^\beta d\tau \int d^3\mathbf{x} \left(\sigma - yM^{-2} \bar{q}_{\Lambda_{\mathrm{AUX}}} q_{\Lambda_{\mathrm{AUX}}} \right)^2 \right\}, \tag{2.13}$$

$$1 = \mathcal{N}^{-1} \int D\pi \exp\left\{ -\frac{1}{2} M^2 \int_0^\beta d\tau \int d^3\mathbf{x} \left(\pi - yM^{-2} i\bar{q}_{\Lambda_{\mathrm{AUX}}} \gamma_5 q_{\Lambda_{\mathrm{AUX}}} \right)^2 \right\}, \tag{2.14}$$

where $\mathcal{N}$ is a irrelevant constant and $\beta \equiv 1/kT$ [*]. Since the compositeness conditions are not imposed, M^2 and y are the arbitrary constants. Of course, the physical quantities should be independent of M^2, y and Λ_{AUX}. We introduced the composite operators whose tensor structures are $\mathbf{1}$ and γ_5, and neglected the others, like the Pagels-Stokar approximation.[26] Using G_1 of (2.4) and the contribution from (2.13) and (2.14), we can write our Lagrangian density $\mathcal{L}_A$ as

$$\mathcal{L}_A = \bar{q} i \slashed{\partial} q + V_a + G_1, \tag{2.15}$$

where

$$V_a = \frac{1}{2} M^{-2} y^2 \left((\bar{q}_{\Lambda_{\mathrm{AUX}}} q_{\Lambda_{\mathrm{AUX}}})^2 + (i\bar{q}_{\Lambda_{\mathrm{AUX}}} \gamma_5 q_{\Lambda_{\mathrm{AUX}}})^2 \right)$$
$$- y(\sigma \bar{q}_{\Lambda_{\mathrm{AUX}}} q_{\Lambda_{\mathrm{AUX}}} + \pi i\bar{q}_{\Lambda_{\mathrm{AUX}}} \gamma_5 q_{\Lambda_{\mathrm{AUX}}}) + \frac{1}{2} M^2(\sigma^2 + \pi^2). \tag{2.16}$$

The ERG evolution is divided into two regions, $\Lambda > \Lambda_{\mathrm{AUX}}$ and $\Lambda < \Lambda_{\mathrm{AUX}}$. In the high energy region $\Lambda > \Lambda_{\mathrm{AUX}}$, $\mathcal{L}_A$ describes a pure fermionic system interacting through G_1. At $\Lambda = \Lambda_{\mathrm{AUX}}$, additional Yukawa interactions and four fermi interactions are switched on. In $\Lambda < \Lambda_{\mathrm{AUX}}$, our model becomes the quark-meson system with G_1. We separate quark fields into the high energy mode and the low energy mode at the scale Λ_{AUX}, and the auxiliary

---

[*] In the following, we choose units such that Boltzmann constant $k = 1$.

fields for mesons are introduced as what is coupled with the low energy mode, $q_{\Lambda_{\rm AUX}}$. We show the $\Lambda_{\rm AUX}$ dependence of the order parameters in §3.

The intermediate scale $\Lambda_{\rm AUX}$ plays almost similar role for k_Φ in the Quark-Meson model,[18] however $\Lambda_{\rm AUX}$ is not an UV cutoff for some effective theory. We solve the ERG flow equations from the sufficiently large cutoff $\Lambda_0 \gg \Lambda_{\rm AUX}$ for each temperature T. In both regions: $p > \Lambda_{\rm AUX}$ and $p < \Lambda_{\rm AUX}$, the gluonic contributions are explicitly evaluated through one gluon exchange term G_1, since we are interested in the influence of the gluon thermal screening effect for the chiral phase transition.

2.3. *Flow equations in the ladder approximation*

Now, let us derive the ERG equation. The flow equation describes the change of the effective average action Γ_Λ under an infinitesimal shift of the infrared momentum cutoff Λ. We start with the construction of Γ_Λ. The generating functional of the connected Green function is

$$W_\Lambda[J] = \ln \int D\bar{q}Dq \exp\{-S_{\rm cut} - S_{\rm bare} + \int_0^\beta d\tau \int d^3\mathbf{x}(\bar{\eta}q - \bar{q}\eta)\}, \qquad (2\cdot17)$$

where $S_{\rm bare}$ is the bare action, i.e. $S_{\rm bare} = \int d\tau d^3\mathbf{x}\mathcal{L}_A$, and $\{\bar{\eta}, \eta\}$ are external sources. The IR cutoff term $S_{\rm cut}$ is introduced for the (anti-)quark fields,

$$S_{\rm cut}[\bar{q}, q] = \int_0^\beta d\tau \int d^3\mathbf{x}\, \bar{q}\Delta^{-1}(-i\partial, \Lambda)q. \qquad (2\cdot18)$$

Here Δ^{-1} is a chiral invariant cutoff operator and has the property,

$$\Delta^{-1}(p, \Lambda) \longrightarrow \begin{cases} 0 & \text{for} \quad p \gg \Lambda \\ \infty & \text{for} \quad p \ll \Lambda. \end{cases} \qquad (2\cdot19)$$

We do not introduce the IR cutoff term for boson fields in this paper since we treat the ladder part only. In the ladder approximation, the bosonic degrees of freedom, σ and π are not integrated in (2·17). So we can forget the infrared problem for mesons at $T < T_c$. The infrared problem originated from the absence of the IR cutoff for gluons can be regularized by introducing a sufficiently small IR cutoff $\Lambda_{\rm IR}$ to the gluon propagator in G_1. However, our results are not affected by $\Lambda_{\rm IR}$, since our ERG evolutions of the effective potential as well as the order parameters are frozen fast when Λ gets smaller than the typical scale for the chiral physics.

The cutoff effective action Γ_Λ is defined by Legendre transformation

$$\Gamma_\Lambda[\Phi] = -W_\Lambda[J] + \int_0^\beta d\tau \int d^3\mathbf{x}J \cdot \Phi + S_{\rm cut}[\Phi], \qquad (2\cdot20)$$

where Φ is given by $\delta W_\Lambda[J]/\delta J$ and we use the shorthand notation of the external sources: $J = \{\bar{\eta}, \eta^{\mathrm{T}}\}$. Note that, since S_{cut} preserves the chiral symmetry, the effective action also respects it.

Differentiating both sides of Eq.(2·17) and using (2·20), we get the ERG equation for the effective average action,[27]

$$\Lambda\frac{d}{d\Lambda}\Gamma_\Lambda[\Phi] = -\frac{1}{2}\mathbf{Str}\left[\Lambda\frac{d}{d\Lambda}\Delta^{-1}\left(\Delta^{-1} + \Gamma_\Lambda^{(2)}\right)^{-1}\right], \tag{2·21}$$

where $\mathbf{Str}$ is super-trace which involves momentum (or coordinate) integration, Matsubara summation, spinor summation and color summation. $\Gamma_\Lambda^{(2)}$ is a second (functional) derivative with respect to the fields $\Phi^{\mathrm{T}} = (q^{\mathrm{T}}, \bar{q})$, i.e.

$$\left(\Gamma_\Lambda^{(2)}\right)_{xy} \equiv \frac{\overrightarrow{\delta}}{\delta\Phi_x^{\mathrm{T}}}\Gamma_\Lambda[\Phi]\frac{\overleftarrow{\delta}}{\delta\Phi_y} . \tag{2·22}$$

We employ the sharp cutoff scheme in this paper since in the smooth cutoff case we must perform the momentum integration with respect to the spatial momenta numerically for each Matsubara mode. We want to avoid such a tiresome and unpractical work. The sharp cutoff limit of Eq. (2·21) can be written as:[28]

$$\Lambda\frac{d}{d\Lambda}\Gamma_\Lambda = -\frac{\Lambda}{2}\mathbf{Str}\left[\frac{\delta(|q| - \Lambda)}{\gamma(\mathbf{q})}\widehat{\Gamma}^{(2)}\left(1 + C\widehat{\Gamma}^{(2)}\right)^{-1}\right], \tag{2·23}$$

where $\widehat{\Gamma}^{(2)}$ is a interaction part of the second derivative of Γ_Λ and $\gamma(\mathbf{q})$ is an inverse propagator:

$$\gamma(\mathbf{q}) \equiv \begin{pmatrix} 0 & \slashed{q} \\ \slashed{q}^{\mathrm{T}} & 0 \end{pmatrix} . \tag{2·24}$$

The infrared cutoff propagator $C(\mathbf{q})$ is given by,

$$C(\mathbf{q}) = \frac{\theta(|q| - \Lambda)}{\gamma(\mathbf{q})}. \tag{2·25}$$

It is known that, in the sharp cutoff case the vertices of the effective action Γ_Λ should be expanded in powers of $|p| \equiv \sqrt{p^2}$ instead of the derivatives ∂_μ.[28] Heaviside θ function in ERG equations is also expanded in terms of $|p|$ as

$$\theta(|p - q| - \Lambda) = \theta(p^2 + 2p \cdot q) = \theta(\hat{p} \cdot q) + \sum\frac{p^n}{n!}\delta^{(n)}(\hat{p} \cdot q), \tag{2·26}$$

where $\hat{p}$ is a unit vector parallel to p. Integrating r.h.s. of the ERG equation(2·23) with respect to the internal momenta q, one can expand it in terms of the momentum scale $|p|$.

9

We approximate the effective action as:

$$\Gamma_\Lambda = \int_0^\beta d\tau \int d^3x \left\{ \bar{q} i \slashed{\partial} q + V(\bar{q}, q, \sigma, \pi) + V_a + G_1 + K(\pi, i\bar{q}\gamma_5 q) \right\}, \qquad (2\cdot27)$$

where $K(\pi, i\bar{q}\gamma_5 q)$ is the higher order term of momentum scale expansion. The explicit form of K is shown later, in (2·38). We neglect the kinetic term of σ, which is not concerned with the analysis here. The potential part $V(\bar{q}, q, \sigma, \pi)$ is a function not only of $S = \bar{q}q$ and $P = i\bar{q}\gamma_5 q$ but also of $\bar{q}_{\Lambda_{\text{AUX}}} q_{\Lambda_{\text{AUX}}}$ and $i\bar{q}_{\Lambda_{\text{AUX}}}\gamma_5 q_{\Lambda_{\text{AUX}}}$, therefore vertices of V have momentum dependence like $\theta(\Lambda_{\text{AUX}} - p)$.

The complexity arising from $\theta(\Lambda_{\text{AUX}} - p)$ can be avoided by dividing the ERG evolution into two regions, i.e. the high energy region $\Lambda > \Lambda_{\text{AUX}}$ and the low energy region $\Lambda < \Lambda_{\text{AUX}}$. In the high energy region, $\bar{q}_{\Lambda_{\text{AUX}}} q_{\Lambda_{\text{AUX}}}$ and $i\bar{q}_{\Lambda_{\text{AUX}}}\gamma_5 q_{\Lambda_{\text{AUX}}}$ do not contribute to r.h.s. of Eq.(2·23) since the supports of $\bar{q}_{\Lambda_{\text{AUX}}}(p)$ and $q_{\Lambda_{\text{AUX}}}(p)$ are restricted to $p < \Lambda_{\text{AUX}} < \Lambda$. Thus we can forget V_a in this region. Next, in the low energy region, we need not distinguish $q_{\Lambda_{\text{AUX}}}(p)$ from $q(p)$ in the vertices of the effective action with external momentums $p_i < \Lambda_{\text{AUX}}$ and of course in the ERG equation (2·23). Hence we can replace $q_{\Lambda_{\text{AUX}}}(p)$ with $q(p)$ by choosing Λ_{AUX} larger than typical scales of the chiral dynamics. Now our prescription is that in the high energy region we solve ERG equation by neglecting V_a term and at $\Lambda = \Lambda_{\text{AUX}}$ we shift the potential $V(\bar{q}, q, \sigma, \pi) \to V(\bar{q}, q, \sigma, \pi) + V_a(\bar{q}_{\Lambda_{\text{AUX}}} = \bar{q}, q_{\Lambda_{\text{AUX}}} = q)$. Hereafter in both regions, we write the arguments of the potential V as S, P, σ and π i.e. $V(S, P, \sigma, \pi)$

We can get the ERG equation for V by substituting the zero modes of the composite operators $S_0 \equiv \int d\tau d^3\mathbf{x} S(x)$ and $P_0 \equiv \int d\tau d^3\mathbf{x} P(x)$[*]. The ERG equation for V can be read,[28]

$$\Lambda \frac{d}{d\Lambda} V = -\frac{\Lambda}{2} \mathbf{Str} \left[\ln \left(\gamma(\mathbf{q}) + V^{(2)} + G_1^{(2)} \right) \right], \qquad (2\cdot28)$$

where $V^{(2)}$ and $G_1^{(2)}$ are the matrices of the second derivative of V and of the four fermi interaction induced by one gluon exchange (2·4) with respect to the (anti-)quark fields respectively.

The derivatives of V with respect to (anti-)quarks can be written as

$$\frac{\overrightarrow{\partial}}{\partial \bar{q}_{I,a}} V \frac{\overleftarrow{\partial}}{\partial q^{J,b}} = \delta_b^a \delta_J^I \frac{\partial}{\partial S} V(S, P) + i\delta_b^a \delta_J^I \gamma_5 \frac{\partial}{\partial P} V(S, P) + \cdots, \qquad (2\cdot29)$$

$$\frac{\overrightarrow{\partial}}{\partial q^{\mathrm{T}I,a}} V \frac{\overleftarrow{\partial}}{\partial \bar{q}_{J,b}^{\mathrm{T}}} = -\delta_a^b \delta_I^J \frac{\partial}{\partial S} V(S, P) - i\delta_b^a \delta_J^I \gamma_5 \frac{\partial}{\partial P} V(S, P) + \cdots, \qquad (2\cdot30)$$

---

[*] For the fermionic theory, we can not insert the zero modes of the fermion fields. Otherwise, the higher vertices which is necessary to produce the bulk structure of the general Green function of the fermions vanish due to the Grassmann nature of fermions.

where we omit the terms generating the non-ladder diagrams in ERG. Thus the matrix $V^{(2)}$ is

$$V^{(2)} = \begin{pmatrix} 0 & \delta_b^a \delta_J^I (V_S + i\gamma_5 V_P) \\ -\delta_a^b \delta_I^J (V_S + i\gamma_5^{\mathrm{T}} V_P) & 0 \end{pmatrix}, \qquad (2\cdot31)$$

where subscripts 'S' and 'P' denote the derivative with respect to $S \equiv \bar{q}q$ and $P \equiv i\bar{q}\gamma_5 q$ respectively, e.g. $\bar{V}_S = \partial \bar{V}/\partial S$. The second functional derivative of the gauge induced four fermi interaction $G_1^{(2)}$ is calculated as:

$$G_1^{(2)} = g^2 \left(D^{-1} \right)_{AB}^{\mu\nu} \begin{pmatrix} T^A \gamma_\nu q \otimes q^{\mathrm{T}} \gamma_\mu^{\mathrm{T}} T^{B\mathrm{T}} & -T^A \gamma_\nu q \otimes \bar{q}\gamma_\mu T^B \\ -T^{A\mathrm{T}} \gamma_\nu^{\mathrm{T}} \bar{q}^{\mathrm{T}} \otimes q^{\mathrm{T}} \gamma_\mu^{\mathrm{T}} T^{B\mathrm{T}} & T^{A\mathrm{T}} \gamma_\nu^{\mathrm{T}} \bar{q}^{\mathrm{T}} \otimes \bar{q}\gamma_\mu T^B \end{pmatrix}. \qquad (2\cdot32)$$

The argument of the gauge coupling constant g is an I.R. cutoff Λ, i.e. leading order in the momentum scale expansion. The ladder contributions to σ channel and π channel are given as follows,

$$-T^A \gamma_\nu q^I \otimes \bar{q}_J \gamma_\mu T^A = -\frac{1}{8N_c^2 N_f} \delta_{\mu\nu} \delta_J^I \delta^{AA} (\bar{q}q + i\gamma_5 \bar{q} i\gamma_5 q) \, \mathbf{1}_c + \cdots, \qquad (2\cdot33)$$

where we use the relation of the generator T^A:

$$(T^A)_i^j (T^A)_k^l = \frac{1}{2} \delta_k^j \delta_i^l - \frac{1}{2N_c} \delta_i^j \delta_k^l, \qquad (2\cdot34)$$

and $\mathbf{1}_c$ is a color unit matrix. Consequently, we find the ladder contribution from the gauge interaction G_1 as:

$$G_1^{(2)} = -\frac{g^2(\Lambda)}{8N_c^2 N_f} \left(D^{-1} \right)_{AA}^{\mu\mu} \begin{pmatrix} 0 & \delta_b^a \delta_J^I (S + i\gamma_5 P) \\ -\delta_a^b \delta_I^J (S + i\gamma_5^{\mathrm{T}} P) & 0 \end{pmatrix}. \qquad (2\cdot35)$$

The trace of the gluon propagator $\mathbf{tr}D^{-1} = (D^{-1})_{AA}^{\mu\mu}$ reduces to a factor

$$\mathbf{tr}D^{-1} = \frac{8}{F} + \frac{16}{G} = \frac{8}{\Lambda^2 + m_L^2 (p_0/|\bar{p}|)} + \frac{16}{\Lambda^2 + m_T^2 (p_0/|\bar{p}|)} \qquad (2\cdot36)$$

for $N_c = 3$, where m_L and m_T are longitudinal component and transverse component of thermal mass respectively. The argument $p_0/|\bar{p}|$ of thermal mass is written in terms of Λ and $\omega_n = (2n+1)\pi T$: $(\sqrt{\Lambda^2/\omega_n^2 - 1})^{-1/2}$ in the ERG flow equation. The bosonic Matsubara frequency is $\omega_n = 2n\pi T$. However, in our analysis, the momentum which flows into G_1 in (2·4) is expected to $(2n+1)\pi T$ because of the derivative expansion. We expand $G_1((2n+1)\pi T + \omega_l)$ in terms of ω_l, which is odd, and include only the leading part: $l = 0$. Inserting Eqs. (2·24), (2·31) and (2·35) to Eq.(2·28), the final expression of the potential part of the ERG equation reduces to

$$\Lambda \frac{\partial}{\partial \Lambda} V = \frac{\Lambda^2 T}{\pi^2} N_f N_c \sum_n{}' \sqrt{\Lambda^2 - \omega_n^2} \ln \left(\Lambda^2 + \bar{V}_S^2 + \bar{V}_P^2 \right), \qquad (2\cdot37)$$

11

where we write $\bar{V} \equiv V - g^2(S^2+P^2)\mathbf{tr}D^{-1}/32N_c^2N_f$ and $\sum_n'$ is a summation over Mastubara modes n with the condition $\Lambda^2 \geq \omega_n^2$. Thus the RG evolution terminates at $\Lambda = \pi T$.

The pion wave function renormalization factors of the spatial derivative and the temporal one are different because the Lorentz invariance is lost. For the derivation of the ERG flow equations for the π wave function renormalization factors, $Z_{\pi L}$ and $Z_{\pi T}$, we consider the higher order contribution of momentum scale expansion in (2·27),

$$K(\pi, P) = \frac{1}{2}Z_\pi(p)\pi_{\mathbf{p}}\pi_{-\mathbf{p}} + Y_\pi(p)\pi_{\mathbf{p}}P_{-\mathbf{p}} + \frac{1}{2}G(p)P_{\mathbf{p}}P_{-\mathbf{p}}, \tag{2·38}$$

where $P_{\mathbf{p}}$ is a pionic composite operator: $P_{\mathbf{p}} = (\bar{q}i\gamma_5 q)_{\mathbf{p}}$, and subscripts $\mathbf{p}$ and $-\mathbf{p}$ denotes their momenta. $Y_\pi(p)$ and $G(p)$ are the momentum dependent vertices of Yukawa interaction and that of four fermi interaction respectively. Taking functional derivative of $K(\pi, P)$ with respect to $P_{\mathbf{p}}$ and $P_{-\mathbf{p}}$, and substituting to (2·23), the ERG equation for K is given by

$$\Lambda\frac{d}{d\Lambda}K(\mathbf{p}) = \frac{\Lambda}{2}\mathbf{Str}\Big[\delta(|q|-\Lambda)\mathbf{S}_F(\mathbf{q})\hat{Y}\theta(|p+q|-\Lambda)\mathbf{S}_F(\mathbf{p+q})\hat{Y}\Big]\frac{\delta\hat{K}}{\delta P_{-\mathbf{p}}}\frac{\delta\hat{K}}{P_{\mathbf{p}}}\theta(\Lambda_{\text{AUX}}-\Lambda). \tag{2·39}$$

$\hat{K}$ denotes the 'interaction parts' of K, where the pion kinetic term is subtracted in (2·38). The step function $\theta(\Lambda_{\text{AUX}} - \Lambda)$ in r.h.s. of Eq.(2·39) is due to the cutoff of the quark-meson interaction. It tells that K contributes to the whole ERG flow for $\Lambda < \Lambda_{\text{AUX}}$. $\mathbf{S}_F$ and $\hat{Y}$ are the massive quark propagator on the vacuum $<\sigma> = \sigma_0$ and the matrix part of the Yukawa coupling constant: $Y_\pi(p) \equiv Y(p)\hat{Y}$ respectively. Introducing the coupling constants $V = m\,\bar{q}q + \cdots$, $\mathbf{S}_F$ is written as:

$$\mathbf{S}_F^{-1}(\mathbf{q}) = \gamma(\mathbf{q}) + \begin{pmatrix} \mathbf{0} & m \\ -m & \mathbf{0} \end{pmatrix}, \tag{2·40}$$

and $\hat{Y}$ is given by,

$$\hat{Y} \equiv \begin{pmatrix} \mathbf{0} & i\gamma_5 \\ -i\gamma_5^{\text{T}} & \mathbf{0} \end{pmatrix}. \tag{2·41}$$

To devive the ERG equation of $Z_{\pi L}$ and $Z_{\pi T}$, we expand (2·39) in powers of momentum scale to second order. Note that, terms which mix p_0 and $\bar{p}$ do not contribute to the wave function renormalization factors. The momentum dependent vertices are expanded as:

$$Z_\pi(p) = Z_{\pi L}p_0^2 + Z_{\pi T}\bar{p}^2 + O(p), \tag{2·42}$$

$$Y(p) = (|p_0|/\Lambda)y_{1L} + (\bar{p}/\Lambda)y_{1T} + (p_0/\Lambda)^2y_{2L} + (\bar{p}/\Lambda)^2y_{2T}, \tag{2·43}$$

$$G(p) = (|p_0|/\Lambda)g_{1L} + (\bar{p}/\Lambda)g_{1T} + (p_0/\Lambda)^2g_{2L} + (\bar{p}/\Lambda)^2g_{2T}. \tag{2·44}$$

12

We need to be careful about expanding the inside of square bracket in (2·39) in terms of p_0, which takes discontinuous value at finite temperature. Let us expand a function $f(p_0)$ as:

$$f(p_0) = f_0 + f_1|p_0| + f_2 p_0^2. \tag{2·45}$$

We estimate the expansion of $f(p_0)$ using three points of bosonic Matsubara frequency, $p_0 = 0$, $p_0 = 2\pi T$ and $p_0 = 4\pi T$, as:

$$4\pi T f_1 = -3f(p_0 = 0) + 4f(p_0 = 2\pi T) - f(p_0 = 4\pi T), \tag{2·46}$$

$$8\pi^2 T^2 f_2 = f(p_0 = 0) - 2f(p_0 = 2\pi T) + f(p_0 = 4\pi T). \tag{2·47}$$

The result of the expansion above becomes identical to that of the ordinary momentum scale expansion at $T \to 0$. Finally, we get following ERG equations,

$$\Lambda \frac{d}{d\Lambda} Z_{\pi(L,T)} = m^2 I_{2(L,T)} + (2my_{2(L,T)} + y_{1(L,T)}^2)I_0 + 2my_{1(L,T)}I_{1(L,T)}, \tag{2·48}$$

$$\Lambda \frac{d}{d\Lambda} y_{1(L,T)} = mg_\sigma I_{1(L,T)} + (y_{1(L,T)}g_\sigma + mg_{1(L,T)})I_0, \tag{2·49}$$

$$\Lambda \frac{d}{d\Lambda} y_{2(L,T)} = mg_\sigma I_{2(L,T)} + (y_{1(L,T)}g_\sigma + mg_{1(L,T)})I_{1(L,T)}$$
$$+ (mg_{2(L,T)} + y_{1(L,T)}g_{1(L,T)} + y_{2(L,T)}g_\sigma)I_0, \tag{2·50}$$

$$\Lambda \frac{d}{d\Lambda} g_{1(L,T)} = g_\sigma^2 I_{1(L,T)} + 2g_\sigma g_{1(L,T)}I_0, \tag{2·51}$$

$$\Lambda \frac{d}{d\Lambda} g_{2(L,T)} = g_\sigma^2 I_{2(L,T)} + 2g_\sigma g_{1(L,T)}I_{1(L,T)} + (2g_\sigma g_{2(L,T)} + g_{1(L,T)}^2)I_0. \tag{2·52}$$

The threshold functions $I_{k(L,T)}$ include Matsubara sum. The explicit forms of $I_{k(L,T)}$ are given in Appendix A. ERG equations for m and g_σ are derived by the polynomial expansion of V in terms of the composite operator. We show the explicit form later.

§3. Numerical Analysis

3.1. *Truncation and Λ_{AUX} dependence of the order parameters*

Before starting the analysis of the chiral phase transition at finite temperature, we investigate the truncation and Λ_{AUX} dependence of the order parameters. In general, the approximate solutions depend Λ_{AUX} since the Λ_{AUX} dependent factors can not be eliminated by the normalization of the redundant degrees of freedom σ, π. Hence the Λ_{AUX} dependence of the results should be verified. In this paper we show the truncation/Λ_{AUX} dependence of the order parameters such as the pion decay constant f_π and the chiral condensate $<\bar{\psi}\psi>$ at zero temperature.

At zero temperature, the ERG flow equation for V reduces to

$$\Lambda\frac{\partial}{\partial\Lambda}V = \frac{1}{4\pi^2}N_f N_c \ln\left(\Lambda^2 + \bar{V}_S^2 + \bar{V}_P^2\right), \tag{3.1}$$

where $\bar{V} \equiv V - 3g^2(S^2 + P^2)/2N_c^2 N_f \Lambda^2$. This flow equation leads to the ladder-exact results for the chiral condensate $<\bar{\psi}\psi>$ and the dynamical quark mass m_{eff}.[15] Here $(\bar{\psi})\,\psi$ denotes the (anti-)quark field with a definite flavor.

To estimate the π decay constant, we must calculate the wave function renormalization factor of the meson fields Z_π. The ERG equations of Z_π and momentum dependent vertices are the same form as (2.48)-(2.52). At zero temperature, there exists no distinction between L and T. The explicit forms of zero temperature coefficients I_k are also given in Appendix A.

The π decay constant f_π is given in terms of Z_π and the vacuum expectation value (VEV) σ_0[18] *) :

$$f_\pi = \sqrt{2/3}Z_\pi^{1/2}\sigma_0. \tag{3.2}$$

The coefficient differs from that in 18) because our normalizations of the auxiliary fields are different. To estimate the chiral condensate, we introduce the external source m_0 for the composite operator $\bar{q}q$. The chiral condensate is given by

$$-<(\bar{\psi}\psi)_{\Lambda_0}> = \frac{1}{N_f}\frac{\partial V(\sigma_0)}{\partial m_0}\bigg|_{m_0=0}, \tag{3.3}$$

where we write the renormalization point Λ_0 since this formula leads the chiral condensate renormalized at U.V. cutoff scale Λ_0. The ERG flow starts from $\Lambda = \Lambda_0$, so the solutions of the ERG depend on Λ_0. In this paper, we set Λ_0 as: $\Lambda_0 = \Lambda_{\text{QCD}} \times e^{10.5}$. Hereafter, we consider the case: $N_f = 3$.

We first investigate the truncation dependence of the order parameters. The potential V is truncated to the $(N-1)$-th polynomial of S,

$$V(S) = \sum_{n=1}^{N} v_{n-1}S^{n-1}, \tag{3.4}$$

where v_n are the VEV σ_0 dependent coefficients. By virtue of the parity invariance, the higher terms of P do not contribute to $O(P^0)$ terms. So we can neglect such terms in (3.4) without losing generality. The ERG flow equation reduces to a coupled ordinary differential equation. The truncation (N) dependence of f_π is shown in Fig.2. As shown in Fig.2, π decay constant rapidly converges against truncation of the effective potential $V(S)$. We set

---

*) We introduced flavor-singlet auxiliary fields by (2.13) and (2.14). In our approximation, the decay constant can be regarded as that of meson flavor-$SU(3)$ octet.

Λ_{QCD} to 583 MeV, so as to the convergent f_π becomes 92.42 MeV, which is the experimental value at $T = 0$.[29] Throughout this paper, Λ_{QCD} is fixed to this value. In this calculation, we choose $\Delta t \equiv \ln(\Lambda_{\text{AUX}}/\Lambda_{\text{QCD}}) = 1.0$.
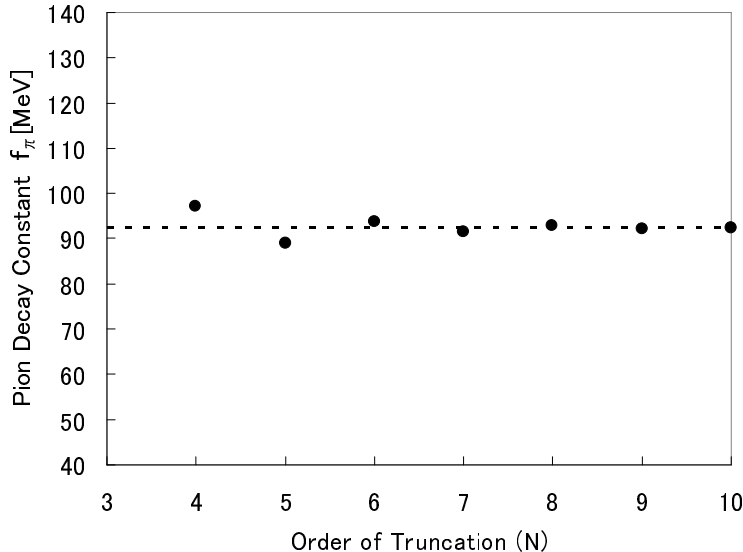

Fig. 2. Truncation dependence of the π decay constant. The dotted line is $f_\pi = 92.42$ MeV. The order of truncation corresponds to N.

In Table I, the truncation dependence of the chiral condensate, the quark dynamical mass and the π decay constant are described. The chiral condensate is renormalized at 1 GeV. Although the chiral condensate and the dynamical quark mass have already been calculated in Ref.15), we show the truncation dependence of these quantities since the results may depend on the unphysical parameters, e.g. Δt, for the lower truncation $N \leq 5$ where the results do not converge yet.

Table I. Truncation dependence of the chiral condensate, the quark dynamical mass and the π decay constant. ψ denotes the quark with a definite flavour.

Truncation (N)	4	5	6	7	8	9	10
$\|<\bar{\psi}\psi>\|^{1/3}$ (MeV)	273.2	258.2	260.8	259.6	260.2	259.9	259.9
m_{eff} (MeV)	1072.4	1084.8	1063.4	1073.1	1068.6	1070.6	1069.8
f_π (MeV)	97.24	88.88	93.70	91.44	92.72	92.13	92.42

Next, we investigate the Λ_{AUX} dependence of the order parameters. The Λ_{AUX} dependence of $<\bar{\psi}\psi>^{1/3}$ and f_π for $N{=}10$ are summarized in Table II and Fig. 3. The chiral condensate is quite stable to Δt. We show the Λ_{AUX} dependence of the pion decay constants in two approximation schemes. In 'Scheme A' we neglect $Y(p)$ and $G(p)$ in (2·38). 'Scheme B' denotes the solution of (2·48)-(2·52). The Λ_{AUX} dependence of π decay constant

15

is considerably decreased by the momentum scale expansion, 20% to 4%. $O(\partial^0)$ quantity $< \bar{\psi}\psi >^{1/3}$ and m_{eff} are stable to the change of Λ_{AUX} in this approximation. The stabilities of these quantities are maintained at finite temperature. For $T \approx 120$ MeV and $N = 6$, Λ_{AUX} dependence of $< \bar{\psi}\psi >^{1/3}$ was estimated 0.5% in the region $\Delta t = [0.5, 1.0]$. Therefore the critical temperature is also stable. Hereafter we choose $\Delta t = 1.0$ and $N = 6$.

Fig. 3. Λ_{AUX} dependence of the π decay constant and the chiral condensate for the truncation $N = 10$.

Table II. Λ_{AUX} dependence of the order parameters.

Δt	0.4	0.5	0.6	0.7	0.8	0.9	1.0
$\| < \bar{\psi}\psi > \|^{1/3}$ (MeV)	260.2	260.1	260.3	260.3	259.9	260.0	260.2
f_π[Scheme A] (MeV)	130.47	131.94	130.17	124.67	117.59	111.69	105.30
f_π[Scheme B](MeV)	94.49	96.65	96.35	95.08	93.50	93.21	92.42

3.2. *Chiral phase transition at high temperature*

Let us analyze the chiral phase transition at high temperature. We first solve the ERG equation for the potential $V(S)$ to estimate the critical temperature and the chiral condensate. The ERG equation for $V(S)$ is already derived in (2·37). Expanding the potential as: $V = v_0 + mS - g_\sigma S^2/2 + G_6 S^3/3 + \cdots$, and substituting to the ERG equation we have

$$\Lambda \frac{d}{d\Lambda} v_0 = \zeta^0 \ln(\Lambda^2 + m^2), \tag{3·5}$$

$$\Lambda \frac{d}{d\Lambda} m = -\frac{2m\zeta^1}{\Lambda^2 + m^2}, \tag{3·6}$$

$$\Lambda \frac{d}{d\Lambda} \left(-\frac{g_\sigma}{2} \right) = \frac{1}{\Lambda^2 + m^2} \left(\zeta^2 + 2mG_6\zeta^0 - \frac{2m^2\zeta^2}{\Lambda^2 + m^2} \right), \tag{3·7}$$

$$\Lambda \frac{d}{d\Lambda}\left(\frac{G_6}{3}\right) = -\frac{2G_6\zeta^1}{\Lambda^2 + m^2} + \frac{2m}{(\Lambda^2 + m^2)^2}\left\{\zeta^3 + 2mG_6\zeta^1 - \frac{8}{3}\frac{m^3\zeta^3}{\Lambda^2 + m^2}\right\}, \qquad (3\cdot8)$$

$$\Lambda \frac{d}{d\Lambda}\left(\frac{G_8}{4}\right) = \cdots, \qquad (3\cdot9)$$

where ζ^l denotes Matsubara frequency sums i.e.

$$\zeta^l = \frac{\Lambda^2 T}{\pi^2} N_c N_f \sum_n{}' \sqrt{\Lambda^2 - \omega_n^2}\left(g_\sigma + g^2\mathbf{tr}D^{-1}/16N_c^2 N_f\right)^l, \qquad (3\cdot10)$$

where $N_f = N_c = 3$.

The temperature dependence of the potential V are shown in Fig.4. The order of phase transition is second order or very weak first order, and the critical temperature in our approximation is found to be 124.1 MeV. This result should be compared with $T_c = 169$ MeV given by Y. Taniguchi and Y. Yoshida,[10] $T_c = 166$ MeV given by M. Harada and A. Shibata[11] and/or $T_c = 129$ MeV proposed by O. Kiriyama, M. Maruyama and F. Takagi.[12] Their analyses do not consider the gluon thermal mass. In Ref.13), the effect of the Debye screening at finite temperature and/or density is studied. The thermal mass is included in the static limit of the HTL approximation, thus the magnetic screening is ignored. T_c gets 147 MeV by this approximation. These works adopt the same running coupling constant $g(p,k)$ at $T = 0$. Furthermore, the angular dependent part of the argument of $g(p,k) = g((p+k)^2)$ was neglected. In our analysis, the higher order terms with respect to $|p|$ are not introduced at present. We consider the leading part of derivative expansion, and the argument of g becomes Λ in our analysis. At $T = 0$, this leading approximation scheme is identical to the prescription $g(p,k) = g(\max(p,k))$ in SDEs.[15]

Next, we estimate the pion decay constants at finite temperature. At finite temperature, there are two distinct π decay constants: the temporal one $f_{\pi L}$ and the spatial one $f_{\pi T}$. They are defined by

$$j_5^0 \sim f_{\pi L}\partial^0\pi + \cdots, \qquad (3\cdot11)$$

$$j_5^i \sim f_{\pi T}\partial^i\pi + \cdots. \qquad (3\cdot12)$$

We can calculate these in terms of the wave function renormalization factor of meson field[*]:

$$f_{\pi L} = \sqrt{2/3}Z_{\pi L}^{1/2}\sigma_0, \qquad f_{\pi T} = \sqrt{2/3}Z_{\pi T}/Z_{\pi L}^{1/2}\sigma_0. \qquad (3\cdot13)$$

The ERG flow equations for $Z_{\pi L}$ and $Z_{\pi T}$ are already derived in (2·48). Solving those equations, and substituting the solutions to (3·13), we gain $f_{\pi L}$ and $f_{\pi T}$.

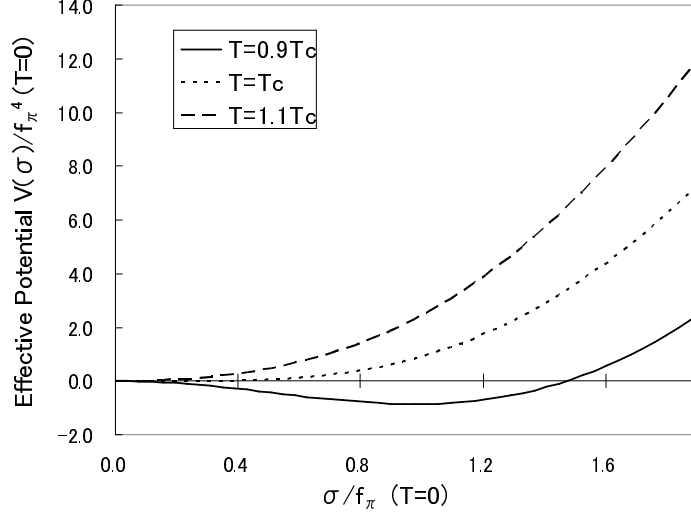[*] We renormalize the pion field as: $\pi_R = Z_{\pi L}^{1/2}\pi$.

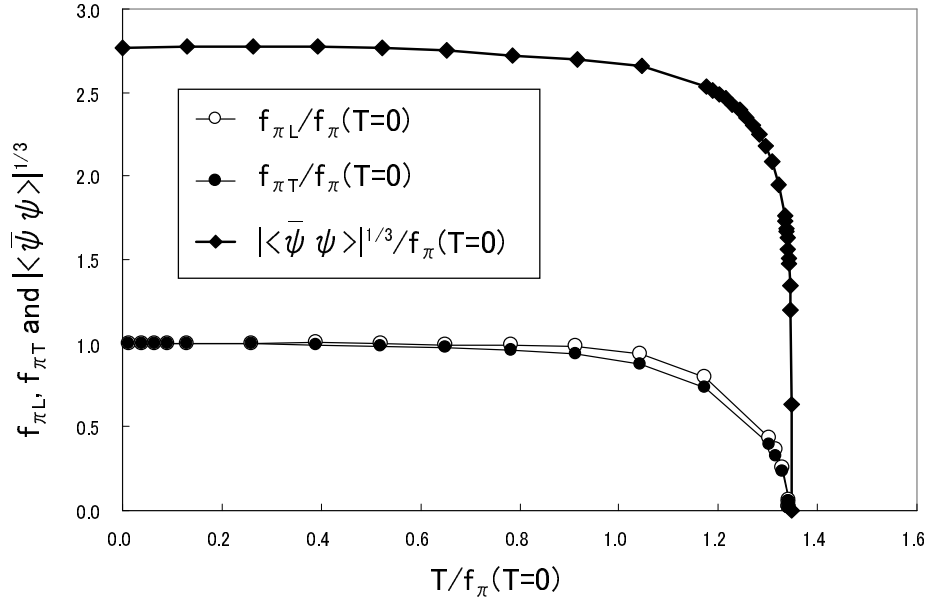Fig. 4. Temperature dependence of the effective potential. The gluon thermal mass is incorporated.

Fig. 5. Temperature dependence of the order parameters.

The chiral condensate $< \bar{\psi}\psi >$ can be evaluated by the common manner with the zero temperature case. The temperature dependence of the order parameters are shown in Fig. 5. $| < \bar{\psi}\psi > |^{1/3}/f_\pi(T=0)$ keeps almost constant value 2.8 at low temperature $T/f_\pi(T=0) \leq$ 0.7 and decreases rapidly at $T/f_\pi(T=0) \geq 1.2$. Finally, $| < \bar{\psi}\psi > |^{1/3}$ vanishes at $T = T_c$. The transverse and longitudinal pion decay constants: $f_{\pi T}$ and $f_{\pi L}$ take almost same value at low temperature. The difference between them is less than 1% for $T/f_\pi(T=0) \leq 0.4$. However, for high temperature over $T/f_\pi(T=0) \geq 0.8$, the difference of two decay constants gradually becomes visible. Here, we can consider pion velocity in the thermal bath. The

18

pion momentum $\bar{p}$ and the pion energy p_0 satisfy the dispersion relation:

$$p_0^2 = \frac{Z_{\pi T}}{Z_{\pi L}}|\bar{p}|^2. \tag{3·14}$$

and pion's squared velocity v^2 is defined from the ratio of pion wave function renormalization factors, or decay constants:

$$v^2 = Z_{\pi T}/Z_{\pi L} = f_{\pi T}/f_{\pi L}. \tag{3·15}$$

The temperature dependence of the pion velocity v is drawn in Fig.6. It shows that pion travels at the velocity of light in the low temperature region, and that it slows down slightly as temperature rises. At $T = T_c$, the pion velocity is slowed down to $v/c \approx 0.95$.

Fig. 6. Temperature dependence of the pion velocity.

Next, we want to know the critical exponents from the temperature dependence of the order parameters. From the construction in sec.2, our effective potential V is invariant under the transformation: $\bar{\psi}\psi \to -\bar{\psi}\psi, m_0 \to -m_0, \sigma_0 \to -\sigma_0$. Thus, the chiral condensate in (3·3) is considered to behave as:

$$< \bar{\psi}\psi > = \sigma_0 f(\sigma_0^2(T)). \tag{3·16}$$

$< \bar{\psi}\psi >$ and σ_0 vanish at $T = T_c$, however, $f(0)$ keeps some finite value. Therefore, the critical exponent of the chiral condensate is derived by

$$| < \bar{\psi}\psi > (T)| \sim C\sigma_0(T) \sim |T - T_c|^\nu, \tag{3·17}$$

where C is some constant. The critical exponents of $f_{\pi L}$ and $f_{\pi T}$ are estimated in the same way. $Z_{\pi L}$ and $Z_{\pi T}$ in (3·13) never go to zero when $T \to T_c$, so the exponents are determined by the temperature dependence of $\sigma_0(T)$, same as in (3·17). The critical exponents for the chiral condensate $< \bar{\psi}\psi >$ and decay constants $f_{\pi L}$ and $f_{\pi T}$ should be universal. The

19

logarithms of $|<\bar{\psi}\psi>|^{1/3}/f_\pi$ and $|T-T_c|/f_\pi$ are plotted in Fig.7. We draw the line, $\log|<\bar{\psi}\psi>|=\nu\log|T_c-T|+C'$, where ν and C' are determined by the ordinary least squares, using the black points in Fig.7. We can find the critical exponent: $\nu=0.48$.
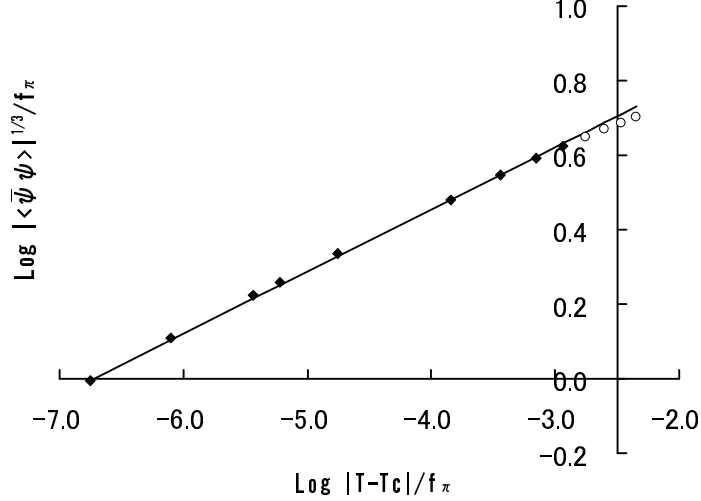

Fig. 7. The relation of $\log|T-T_c|/f_\pi$ and $\log|<\bar{\psi}\psi>|^{1/3}/f_\pi$. The black points are the datum used in the linear regression, and the white ones are not used.

At zero temperature, it is verified that physical quantities do not depend too much on the choice of the IR regularization of the running coupling constant.[7] So we similarly need to examine the Λ_1 dependence of T_c to guarantee the confidence of our results. In Ref.13), $t_f=\ln(\Lambda_1/\Lambda_{\rm QCD})^2$ dependence of the numerical results for the QCD phase structure is also discussed. It is shown that T_c at $\mu=0$ are stable for $t_f=0.6, 0.5$, and 0.4. In our calculation we find $T_c=120$ MeV, 124 MeV, and 129 MeV for $t_f=0.6, 0.5$, and 0.4 respectively.

3.3. *Approximation scheme for the thermal mass*

So far, we carry out the calculations at finite temperature introducing the gluon thermal mass in the HTL approximation. This is the most striking difference from many previous works in the SDEs. There are several attempts to introduce the gluon thermal mass. We finally carry out the calculation in other approximations, and show how the difference is reflected to the result. In Table III, we compare our result with other approximation schemes for the thermal screening effect.

The values 'HTL approx' in Table III are our results and the case labeled '$p_0/|\bar{p}|$ leading' is the well known form of the Landau damping,[24]

$$m_L^2=\frac{1}{3}g^2T^2\left(N_c+\frac{1}{2}N_f\right), \qquad m_T^2=\frac{\pi}{4}m_L^2\frac{|p_0|}{|\bar{p}|}. \tag{3.18}$$

This approximation has been applied to investigate the color superconductivity at high

Table III. The critical temperature and the critical exponent in several approximations.

Scheme	T_c (MeV)	ν
HTL approx.	124.1	0.48
$|p_0|/|\bar{p}|$ leading	98.6	0.47
Static limit of HTL	154.3	0.50
Neglected	171.9	0.50

density.[30] Third one is the static limit of the HTL approximation,[8],[13] i.e.

$$m_L^2 = \frac{1}{3}g^2T^2\left(N_c + \frac{1}{2}N_f\right), \qquad m_T^2 = 0. \tag{3·19}$$

In the last case, the screening effect are dropped:

$$m_L^2 = m_T^2 = 0. \tag{3·20}$$

In Ref.11) and Ref.12), the chiral phase transition at finite temperature/density has discussed in this approximation. T_c in the second case is the lowest in our results. It is supposed that the factor $|p_0|/|\bar{p}|$ in (3·18) causes large m_T for small $|\bar{p}|$ (or large p_0) and strong screening effects. The critical exponents in the third case and the last case are found to be $\nu = 0.50$. It seems that the critical exponent, at least in our approximation, depends on the treatment of the magnetic mass. The deviation from our result are at most 4% for the critical exponent, while $20 \sim 40\%$ for the critical temperature. The temperature dependences of the order parameters for each method are shown below. In Fig.8, the temperature dependences of $|<\bar{\psi}\psi>|^{1/3}$ is plotted. It tells us that the difference by approximation for the thermal mass appears at $T/f_\pi(T = 0) \geq 0.4$. In each case $|<\bar{\psi}\psi>|^{1/3}$ begins to decrease at $T/f_\pi(T = 0) \approx T_c/f_\pi(T = 0) - 0.4$, and rapidly goes to zero over $T/f_\pi(T = 0) \approx T_c/f_\pi(T = 0) - 0.1$.

In Fig.9, we plot $f_\pi(T)/f_\pi(T = 0)$, where $f_\pi(T)$ is so-called 'space-time averaged' decay constant,[11] defined by $f_\pi(T) \equiv (f_{\pi L}^2 + 3f_{\pi T}f_{\pi L})^{1/2}/2$. It tells that the effects of the thermal mass appear at $T/f_\pi(T = 0) \geq 0.4$. There is a definite peak in the 'Neglected' case. In SDEs, the temperature dependence of $f_\pi(T)$ is estimated, not that of $f_{\pi L}$ and $f_{\pi T}$ one by one.[11] In Ref.11), the dependence is calculated by neglecting the thermal mass and there is a peak at $T/f_\pi(T = 0) \approx 1.2$.

The quantitative difference becomes evidently for the pion velocity v. In Fig.10, the difference of how v is slowed down is plotted. v/c is finally reduced to $0.92, 0.92, 0.95$, and 0.95 for 'Neglected', 'Static limit', 'HTL', and '$|p_0|/|\bar{p}|$ leading' respectively at each T_c. v_c at $T = T_c$ hardly depend on T_c. It tells that v/c at T_c depends obviously whether magnetic

mass is introduced or not. There are peaks in the 'Neglected' case and 'Static limit' case, and in the former case, v/c is increased to about 1.00 again near $T/f_\pi(T=0) = 0.9$.
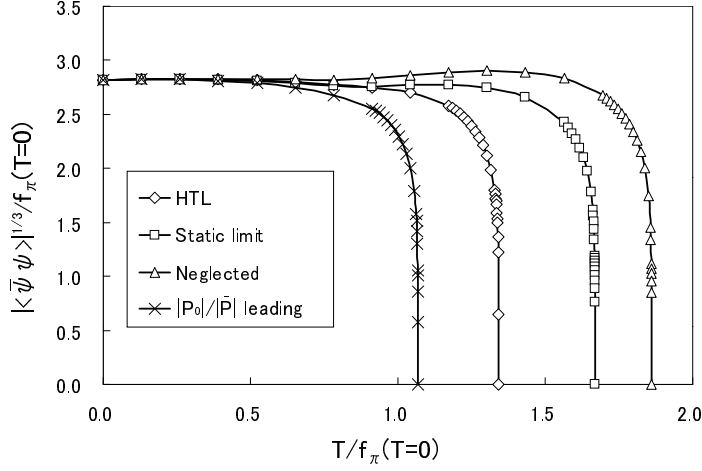

Fig. 8.   Temperature dependence of $| < \psi\bar{\psi} > |$ for each scheme.
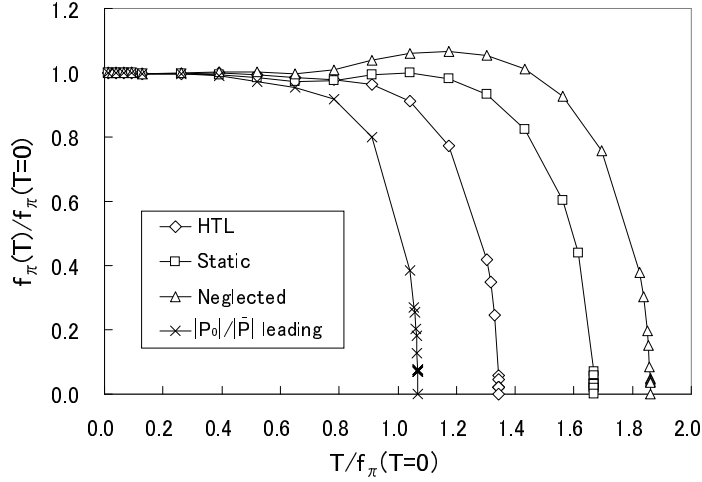

Fig. 9.   Temperature dependence of $f_\pi(T)/f_\pi$ for each scheme.

§4.   Summary and Discussions

In this paper we analyzed the chiral phase structure of finite temperature QCD for 3-flavors by solving the sharp cutoff ERG flow equation. We derived the equation in the ladder approximation. The auxiliary fields σ and π were introduced at the scale Λ_{AUX}, which is larger than Λ_{QCD}. It was shown that the dependence of f_π on Λ_{AUX} was considerably improved by the momentum scale expansion. The gluon thermal mass is incorporated by the HTL approximation. As a result the critical temperature T_c has become about 124 MeV, which is considerably lower value than the one calculated by neglecting the thermal mass. We
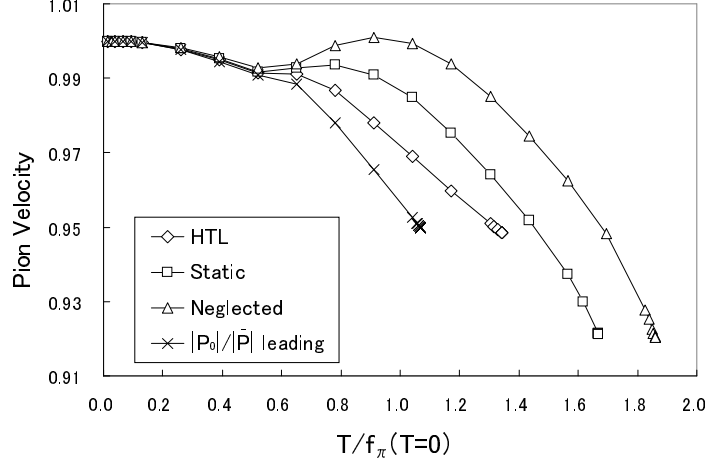
22

Fig. 10. Temperature dependence of pion velocity v for each scheme.

also make certain that T_c and the temperature dependence of the order parameters depend on the approximation scheme for the thermal mass. Our result shows that the screening effect is an important factor when the chiral phase structure of finite temperature QCD is discussed.

In this paper, we replaced the gauge sector with the momentum dependent four fermi operator induced by one gluon exchange. Of course, the gauge dynamics in finite temperature QCD can be incorporated solely by the ERG. Then we have to employ the gauge invariant ERG[21] or MSTI.[20] As mentioned in §2, both attempts will demand too much effort of human as well as machines.

Including the instanton effect is the one of the interesting extensions of this work. There are various possible scenarios about the connection between $U(1)_A$ symmetry and the chiral phase transition.[31]   However, in the ERG framework $U(1)$ symmetry breaking can not be incorporated straightforwardly because of the IR cutoff.[32]   To study the effect of the anomaly, we have to add the instanton induced multi fermi term to Γ_Λ at the initial scale.

The phase transition seems to be second order, or very weak first order. We also studied the temperature dependence of the order parameters for each approximation scheme for the thermal mass. In the HTL, the chiral condensate and two π decay constants $f_{\pi L}$ and $f_{\pi T}$ vanished for $T \approx 124$ MeV ($T/f_\pi(T = 0) \approx 1.34$), that is the critical temperature. When $T = 0$, $f_{\pi L}$ and $f_{\pi T}$ have the same value. However, as temperature rises higher than $T/f_\pi(T = 0) \approx 0.8$ and approaches T_c, the difference becomes evident. The pion velocity v is determined from the ratio of the decay constants, and it decreases slightly as temperature approaches T_c.

It is one of the attractive subjects to apply our method to the case of finite density. In the passed few years, it has been clarified that the vacuum of hot/dense QCD has rich

23

structure, e.g. color super conducting phase, color-flavor locking phase, and so on.[33] The application of our method to the finite density case seems to be straightforward.

Needless to say, HTL is based on perturbative QCD and it can not be said that this is truly proper method in the temperature region for the chiral phase transition, at most $T \approx 100$ MeV. However, this is just our first step of the exploration of the QCD phase structure by ERG.

Acknowledgments

We would like to thank H. Kodama for the collaboration in the early stage.

Appendix A
—— *Thermal Threshold Functions* ——

In this appendix we give the explicit form of thermal threshold functions $I_{k(L,T)}$ in (2·48)-(2·52). First, we show what corresponds to the $O(p^0)$ component and that of the spatial components.

$$I_0 = 2N_f N_c \frac{T}{\pi^2} {\sum_n}' \sqrt{\Lambda^2 - \omega_n^2} \frac{1}{(\Lambda^2 + m^2)}, \tag{A·1}$$

$$I_{1T} = N_f N_c \frac{\Lambda T}{\pi^2} {\sum_n}' \frac{\omega_n^2 + m^2}{(\Lambda^2 + m^2)^2}, \tag{A·2}$$

$$I_{2T} = -\frac{2}{3} N_f N_c \frac{\Lambda^2 T}{\pi^2} {\sum_n}' \sqrt{\Lambda^2 - \omega_n^2} \frac{\Lambda^2 + 3m^2 + 2\omega_n^2}{(\Lambda^2 + m^2)^3} \tag{A·3}$$

The temporal threshold functions are a little complicated because of discretized expansion (2·46) and (2·47). I_{1L} and I_{2L} are given by

$$I_{1L} = N_f N_c \frac{\Lambda T}{\pi^2} {\sum_n}' \sqrt{\Lambda^2 - \omega_n^2} \left(2 \frac{|\omega_n|}{(\Lambda^2 + m^2)^2} - \frac{J_1}{2\pi T} \right)$$
$$+ N_f N_c \frac{\Lambda}{\pi^3} \sqrt{\Lambda^2 - \pi^2 T^2} K_1, \tag{A·4}$$

$$I_{2L} = N_f N_c \frac{\Lambda^2 T}{\pi^2} {\sum_n}' \sqrt{\Lambda^2 - \omega_n^2} \left(-\frac{|\omega_n|}{2\pi T (\Lambda^2 + m^2)} J_1 + \frac{1}{4\pi^2 T^2} J_2 \right)$$
$$- N_f N_c \frac{\Lambda^2}{\pi^3} \sqrt{\Lambda^2 - \pi^2 T^2} \left(\frac{\pi T}{(\Lambda^2 + m^2)} K_1 - \frac{1}{2\pi T} K_2 \right), \tag{A·5}$$

$$\tag{A·6}$$

24

where J_1, J_2, K_1 and K_2 are defined as:

$$J_1 \equiv \frac{3}{\Lambda^2 + m^2} - \frac{4}{\Lambda^2 + m^2 + 4\pi T \omega_n + 4\pi^2 T^2} + \frac{1}{\Lambda^2 + m^2 + 8\pi T \omega_n + 16\pi^2 T^2}, \quad \text{(A·7)}$$

$$J_2 \equiv \frac{1}{\Lambda^2 + m^2} - \frac{1}{\Lambda^2 + m^2 + 4\pi T \omega_n + 4\pi^2 T^2} + \frac{1}{\Lambda^2 + m^2 + 8\pi T \omega_n + 16\pi^2 T^2}, \quad \text{(A·8)}$$

$$K_1 \equiv \frac{2}{\Lambda^2 + m^2} - \frac{1}{\Lambda^2 + m^2 + 8\pi^2 T^2}, \quad \text{(A·9)}$$

$$K_2 \equiv -\frac{1}{\Lambda^2 + m^2} + \frac{1}{\Lambda^2 + m^2 + 8\pi^2 T^2}. \quad \text{(A·10)}$$

At $T = 0$, I_{kL} and I_{kT} reduce to an identical form. They are given by

$$I_0 = \frac{\Lambda^2}{2\pi^2} \frac{1}{\Lambda^2 + m^2}, \quad \text{(A·11)}$$

$$I_1 = \frac{\Lambda^2}{3\pi^3} \frac{\Lambda^2 + 3m^2}{(\Lambda^2 + m^2)^2}, \quad \text{(A·12)}$$

$$I_2 = -\frac{\Lambda^4}{4\pi^2} \frac{\Lambda^2 + 2m^2}{(\Lambda^2 + m^2)^3}. \quad \text{(A·13)}$$

References

1) Y. Nambu and G. Jona-Lasinio, Phys. Rev. **122** (1961), 345.
   T. Maskawa and H. Nakajima, Prog. Theor. Phys. **52** (1974), 1326.
   R. Fukuda and T. Kugo, Nucl. Phys. **B117** (1976), 250. V. A. Miransky, Nuovo Cim. **90A** (1985), 149.

2) K.-I. Kondo, H. Mino and K. Yamawaki, Phys. Rev. **D39** (1989), 2430.
   K. Yamawaki, *in Proc. Johns Hopkins Workshop on Current Problems in Particle Theory 12, Baltimore, 1988*, eds. G. Domokos and S. Kovesi-Domokos (World Scientific, Singapore, 1988).
   T. Appelquist, M. Soldate, T. Takeuchi and L.C.R. Wijewardhana, ibid.
   W. A. Bardeen, C. N. Leung and S. T. Love, Phys. Rev. Lett. **56** (1986), 1230.
   C. N. Leung, S. T. Love and W. A. Bardeen, Nucl. Phys. **B273** (1986), 649.

3) T. Kugo, "Basic concepts in dynamical symmetry breaking and bound state problems", in Lecture delivered at 1991 Nagoya Spring School on Dynamical Symmetry Breaking, Nakatsugawa, Japan, Apr 23-27, 1991.
   C. D. Roberts and S. M. Schmidt, Prog. Part. Nucl. Phys. 45, (2000) S1.

4) V. A. Miransky, *Dynamical symmetry breaking in quantum field theories* (World Scientific, 1993) 533p.

5) V. A. Miransky, Yad. Fiz. **38** (1983), 468. [Sov. J. Nucl. Phys. **38** (1983), 468.]
   K. Higashijima, Phys. Rev. **D29** (1984), 1228.

6) K-I. Aoki, T. Kugo and M. G. Mitchard, Phys. Lett. **B266** (1991), 467.

K-I. Aoki, M. Bando, T. Kugo, M. G. Mitchard and H. Nakatani, Prog. Theor. Phys. **84** (1990), 683.

7) K-I. Aoki, M. Bando, T. Kugo, and M. G. Mitchard, Prog. Theor. Phys. **85** (1991), 355.

8) K-I. Kondo and K. Yoshida, Int. J. Mod. Phys. **A10** (1995), 199.

K. Fukazawa, T. Inagaki, S. Mukaigawa and T. Muta, Prog. Theor. Phys. **105** (2001), 979.

9) Y. Fueki, H. Nakkagawa, H. Yokota and K. Yoshida, Prog. Theor. Phys. **110** (2003), 777.

10) Y. Taniguchi and Y. Yoshida, Phys. Rev. **D55** (1997), 2283.

11) M. Harada and A. Shibata, Phys. Rev. **D59** (1999), 4010.

12) O. Kiriyama, M. Maruyama and F. Takagi, Phys. Rev. **D62** (2000), 5008.

13) S. Takagi, Prog. Theor. Phys. **109** (2003), 233.

14) Y. Fueki, H. Nakkagawa, H. Yokota and K. Yoshida, Prog. Theor. Phys. **107** (2002), 759.

15) K-I. Aoki, K. Morikawa, J-I. Sumi, H. Terao and M. Tomoyose, Phys. Rev. **D61** (2000), 5008.

16) K-I. Aoki, M. Bando, T. Kugo, K. Hasebe and H. Nakatani,Prog. Theor. Phys. **81** (1989), 866.

17) K-I. Aoki, K. Morikawa, W. Souma, J-I. Sumi, and H. Terao, Prog. Theor. Phys. **102** (1999), 1151.

18) U. Ellwanger and C. Wetterich, Nucl. Phys. **B423** (1994), 137.

J. Berges, N. Tetradis and C. Wetterich, Phys. Rept. **363** (2002), 223, and the refferences therein.

19) R. D. Pisarski and M. Tytgat, Phys. Rev. **D54** (1996), 2989.

20) C. Becchi, *On the construction of renormalized quantum field theory using renormalization group techniques*, in: Elementary Particles, Field Theory and Statistical Mechanics, eds. M. Bonini, G. Marchesini, and E. Onofri, Parma University, 1993.

U. Ellwanger, Phys. Lett. **B335** (1994), 364.

U. Ellwanger, M. Hirsch and A. Weber, Z.Phys. **C69** (1996), 687.

M. Bonini, M. D'Attanasio and G. Marchesini, Nucl. Phys. **B418** (1994), 81; ibid. **421** (1994), 429; ibid. **437** (1995), 163; Phys. Lett. **B346** (1995), 87.

M. D'Attanasio and T. R. Morris, Phys. Lett. **B378** (1996), 213.

F. Freire and C. Wetterich, Phys. Lett. **B380** (1996), 337.

21) T. R. Morris, in *The Exact Renormalization Group*, Eds Krasnitz et al, World Sci

(1999), 1.

T. R. Morris, Nucl. Phys. **B573** (2000), 97.

T. R. Morris, J. High Energy Phys. **0012** (2000), 12.

T. R. Morris, Int. J. Mod. Phys. **A16** (2001), 1899.

S. Arnone, A. Gatti, and T. R. Morris, Phys. Rev. **D67** (2003), 5003.

22) E. Meggiolaro and C. Wetterich, Nucl. Phys. **B606** (2001), 337.

23) T. Kugo and M. Mitchard, Phys. Lett. **B282** (1992), 162; ibid **286** (1992), 355.

24) M. Le Bellac, *Thermal Field Theory* (Cambridge Monographs on Mathematical Physics, 1996).

25) A. Bardeen, C. T. Hill and M. Linder, Phys. Rev. **D41** (1990), 1647.

26) H. Pagels and S. Stokar, Phys. Rev. **D20** (1979), 2947.

27) C. Wetterich, Phys. Lett. **B301** (1993), 90.

M. Bonini, M. D'Attanasio and G. Marchesini, Nucl. Phys. **B409** (1993), 441.

28) T. R. Morris, Int. J. Mod. Phys. **A9** (1994), 2411; Nucl. Phys. **B458** (1996), 477.

T. R. Morris and J. F. Tighe, J. High Energy Phys. **08** (1999), 7.

29) C. Caso et al. (the Particle Data Group), Eur. Phys. J. **C3** (1998), 1.

30) D. K. Hong, V. A. Miransky, I. A. Shovkovy and L. C. R. Wijewardhana, Phys. Rev. **D61** (2000), 6001[Errata; **D62** (2000), 9903].

V. A. Miransky, I. A. Shovkovy and L. C. R. Wijewardhana, Phys. Lett. **B468** (1999), 270; Phys. Rev. **D62** (2000), 5025; Phys. Rev. **D63** (2001), 6005; Phys. Rev. **D64** (2001), 6002.

V. A. Miransky, G. W. Semenoff, I. A. Shovkovy and L. C. R. Wijewardhana, Phys. Rev. **D64** (2001), 5005.

H. Abuki, T. Hatsuda and K. Itakura, Phys. Rev. **D65** (2002), 4014.

31) E. Meggiolaro, Expanded version of a talk given at the "Workshop on Quark-Gluon Plasma and Relativistic Heavy Ions", Frascati (Italy), January 14th-18th, 2002 (QGP2002).

M. Marchi and E. Meggiolaro, Nucl. Phys. **B665** (2003), 425.

32) J. M. Pawlowski, Phys. Rev. **D58** (1998), 5011.

33) see for example, K. Rajagopal and F. Wilczek, To appear as Chapter 35 in the Festschrift in honor of B. L. Ioffe, *At the Frontier of Particle Physics / Handbook of QCD* , M. Shifman, ed., (World Scientific), hep-ph/0011333.